HHS Public Access

Author manuscript

Neuron. Author manuscript; available in PMC 2016 April 22.

Published in final edited form as:

Neuron. 2015 April 22; 86(2): 529–540. doi:10.1016/j.neuron.2015.03.010.

Circuit Mechanisms Underlying Motor Memory Formation in the Cerebellum

Ka Hung Lee[†,1], **Paul J. Mathews**[†,1], **Alexander M.B. Reeves**[1], **Katrina Y. Choe**[1], **Shekib A. Jami**[1], **Raul E. Serrano**[2], and **Thomas S. Otis**[1,*]

[1]Department of Neurobiology and Integrated Center for Learning and Memory, Geffen School of Medicine at UCLA, 650 Charles E. Young Dr., Los Angeles, CA 90095

[2]Department of Physiology, Geffen School of Medicine at UCLA, 650 Charles E. Young Dr., Los Angeles, CA 90095

SUMMARY

The cerebellum stores associative motor memories essential for properly timed movement; however, the mechanisms by which these memories form and are acted upon remain unclear. To determine how cerebellar activity relates to movement and motor learning, we used optogenetics to manipulate spontaneously firing Purkinje neurons (PNs) in mouse simplex lobe. Using high-speed videography and motion tracking, we found that altering PN activity produced rapid forelimb movement. PN inhibition drove movements time-locked to stimulus onset, whereas PN excitation drove delayed movements time-locked to stimulus offset. Pairing either PN inhibition or excitation with sensory stimuli triggered the formation of robust, associative motor memories; however, PN excitation led to learned movements whose timing more closely matched training intervals. These findings implicate inhibition of PNs as a teaching signal, consistent with a model whereby learning leads first to reductions in PN firing that subsequently instruct circuit changes in the cerebellar nucleus.

*Corresponding author. otist@ucla.edu.
†Co-first Authors

AUTHOR CONTRIBUTIONS

K.H.L., P.J.M., A.M.B.R., K.Y.C., and T.S.O. designed experiments. K.H.L. performed the initial experiment observing forelimb movement to launch the project and the surgery and behavioral learning experiments in Figures 3, 4, and 6. P.J.M. performed *in vivo* and *in vitro* recordings, made behavioral kinematic measurements with S.A.J., and generated the histological reconstructions with A.M.B.R. and K.Y.C. K.Y.C. conducted behavioral training on paired and unpaired mice as well as performed the histology and analysis of data in Figures 5 and S7. A.M.B.R. performed the augmentation experiment in Figure 7, wrote Igor routines used to analyze data in Figures 3-6, and analyzed the data in Figures 7, S5, and S6. R.E.S. designed the custom software for acquisition and analysis of the behavioral data. P.J.M. and T.S.O. wrote the manuscript with help from K.H.L, K.Y.C, and A.M.B.R. Given the equal contributions made by K.H.L. and P.J.M., the first author position was determined by a coin flip.

INTRODUCTION

To ensure coordination, the brain must make accurate predictions about how to direct movement (Medina, 2011). These predictions are constructed through a process of error-driven learning, and then stored as associative memories in the cerebellum (Albus, 1971; Marr, 1969; Medina, 2011; Raymond et al., 1996). Correlates of such memories have been observed in the firing patterns of cerebellar Purkinje neurons (PN) as sensory-evoked reductions in the firing rate of PNs in advance of a learned movement (Jirenhed et al., 2007; Lisberger et al., 1994a; Medina and Lisberger, 2008). PNs show high rates of spontaneous activity causing them to powerfully inhibit cerebellar nuclear and vestibular neurons (CNNs) which function as premotor neurons (Person and Raman, 2012). Thus, reductions in spontaneous PN firing in response to the predictive sensory stimulus could, in principle, drive learned movements. Although this disinhibition hypothesis was first suggested four decades ago (Albus, 1971), it is still actively debated (De Zeeuw et al., 2011; Heck et al., 2013; Ito, 1984; Medina, 2011), in part because PN firing patterns do not straightforwardly encode aspects of movement (Cao et al., 2012; Catz et al., 2008; Greger et al., 2004; Kojima et al., 2010; Popa et al., 2013). Moreover, evidence causally linking specific patterns of PN activity to discrete movements has been lacking until very recently (Heiney et al., 2014).

Learning-related changes in PN firing are a hallmark of associative, cerebellum-dependent motor learning, and stimulus induced reductions in PN firing are proposed to play a key role in learning involving increases in movement (Hesslow and Ivarsson, 1994; Jirenhed et al., 2007; Lisberger et al., 1994a; Medina and Lisberger, 2008). Learning is also hypothesized to involve plasticity downstream of PNs within the cerebellar nuclei (Lisberger et al., 1994b; Miles and Lisberger, 1981; Ohyama and Mauk, 2001; Ohyama et al., 2006; Perrett et al., 1993). Evidence from a variety of learning models suggests that associative memory formation occurs in two stages, with circuit changes occurring first in the cerebellar cortex, followed by later changes in the cerebellar nuclei (Cooke et al., 2004; Kassardjian et al., 2005; Ohyama and Mauk, 2001; Okamoto et al., 2011; Shutoh et al., 2006; Titley et al., 2007). In this scenario, learning-related reductions in PN firing could serve to instruct changes in the cerebellar nuclei, leading for example to strengthening of excitatory inputs to CNNs (Maiz et al., 2012b; Mauk, 1997; Mauk and Donegan, 1997; Medina, 2011; Medina and Lisberger, 2008; Ohyama and Mauk, 2001; Otis et al., 2012). At a cellular level, disinhibition of CNNs is known to induce activity-dependent forms of long-term potentiation that could support this type of learning (Pugh and Raman, 2006). Also consistent with this idea, genetic deletion of $GABA_A$ receptors in PNs results in a memory consolidation defect (Wulff et al., 2009), supporting the notion that inhibition-induced pauses in PN firing are required for the formation of cerebellar memories.

In order to determine how PN firing relates to movement and to explore whether certain patterns of PN activity could drive the formation of associative motor memories we developed a behavioral paradigm allowing direct manipulation of PN firing and precise measurement of forelimb movements. We find that inhibiting PNs drives short latency forelimb movements while exciting PNs results in forelimb movements delayed to the offset of excitation, results similar to those described recently for postural movements (Witter et al., 2013). Optrode experiments indicate that in both circumstances movement is linked to

pauses in PN firing and bursts in downstream CNNs. By pairing PN activity with auditory tones, we demonstrate robust associative learning leading to tone-evoked, predictive forelimb movements. Such learning is accompanied by extensive structural plasticity in the cerebellar nuclei. As suggested by a two-stage model, pairing with either excitation or inhibition of PNs drives learning, but the timing of learned movements trained by PN inhibition is less predictive of the training interval, consistent with observations that plasticity in the cerebellar cortex is required for well-timed, learned movements. These findings demonstrate that reductions in PN firing are sufficient to elicit discrete movements and that repeatedly pairing such reductions with sensory stimuli leads to the formation of associative motor memories, implicating inhibition of PNs as an instructive mechanism for driving learning related changes in the cerebellar nuclei.

RESULTS

To examine the underlying mechanisms by which PNs contribute to movement and associative motor memory formation, we exploited Cre-conditional transgenic mice to direct expression of the excitatory opsin ChannelRhodopsin-2 fused to eYFP (ChR2) or the inhibitory opsin Archaerhodopsin-3 fused to eGFP (Arch) in PNs. Expression of ChR2 or Arch was selective for PNs throughout the cerebellum and was apparent in axons projecting to CNNs (Figure 1A and S1). Electrophysiological experiments in brain slices showed that ChR2 activation generates large inward currents and rapid increases in PN firing followed by brief pauses in spontaneous firing activity, while Arch activation generates large outward currents and pauses in the spontaneous firing of PNs (Figure S2). Light-evoked responses and fluorescence were absent from other types of neurons in the cerebellar cortex such as molecular layer interneurons, granule cells, and Golgi cells.

Inhibition of spontaneously firing PNs drives movement

To examine behavioral consequences of transient modulation of PN activity, we developed an awake, head-fixed mouse preparation amenable to simultaneous opsin excitation and extracellular recording. Activation of ChR2 for 75 ms led to robust increases in the simple spike (SSp) firing frequency of PNs (Figure 1B, left, peak freq. = 363.4 ± 40.7 Hz, n=11), and in most PNs the increase was followed by pauses in SSps occurring upon cessation of laser illumination (pause duration 35.0 ± 4 ms in n=9/11 PNs). Recordings of downstream CNN firing showed that ChR2-mediated activation of PNs strongly inhibits CNNs during laser illumination, and that large increases in firing rate occur upon cessation of the laser pulse (Figure 1C, left, peak freq. = 275.3 ± 40.6 Hz, n = 18). In contrast to the ChR2 results, inhibiting PNs via Arch rapidly silenced PN SSp activity (Figure 1B, right, pause duration 99.1 ± 7.4 ms, n= 16) and strongly excited CNNs (Figure 1C, right, peak freq. = 219.6 ± 42.4 Hz, n = 15) during laser illumination. Statistical comparison of peak ChR2-driven rebound firing and peak Arch-driven firing in CNNs indicated no significant differences ($p = 0.33$, two-tailed, paired t-test). Systematically varying pulse duration demonstrated that Arch stimulation led to CNN firing that was time locked to the onset of illumination, while ChR2 stimulation led to CNN inhibition followed by excitation upon offset of laser illumination (Figure S3). Taken together, these findings indicate that the firing frequencies of PNs and

CNNs are robustly and differentially modulated by optogenetic stimuli, and that briefly inhibiting PNs is sufficient to produce high frequency firing of CNNs.

To test whether manipulation of PN/CNN excitability generates motor output we stereotaxically implanted optical fibers in the forelimb motor region of the anterior cerebellar lobe (Figure S1). Movement of the forelimb was monitored in head-fixed mice and measured using high-speed videography (Chettih et al., 2011; Heiney et al., 2014) and motion tracking analysis (Figure 2 and Movie S1). Inhibiting PNs via activation of Arch led to rapid and stereotyped upward forelimb movements during laser illumination that reached peak velocities of 0.3 to 1.5 m/s (Figures 2 and S4). By comparison, excitation of PNs via ChR2 led to delayed movement of similar speed and magnitude, but with onsets time-locked to the laser pulse termination (Figures 2 and S4). This relationship between stimulus onset/offset and movement onset can be visually compared by viewing Movie S2. Across animals, the average timing relative to laser illumination of peak CNN firing and peak movement speed in the two mouse lines indicates that by driving CNN firing, PN pauses lead to the observed forelimb movements (Figure 2D).

Robust motor memories are induced by pairing PN activation with auditory tones

Cerebellum-dependent, associative motor learning has been hypothesized to involve forms of synaptic plasticity triggered by teaching signals from olivo-cerebellar climbing fibers at multiple sites within the cerebellar circuit (Maiz et al., 2012a; Medina and Lisberger, 2008; Raymond et al., 1996), yet the mechanisms underlying this learning are under active debate (Ke et al., 2009; Medina, 2011; Schonewille et al., 2011). Since both climbing fiber-dependent and -independent PN plasticity rely on PN depolarization, we tested whether synchronous PN depolarization can serve as a teaching signal. ChR2 mice were trained by pairing 2-kHz tones with pulses of laser illumination (75-100 ms) delivered 250 ms after tone onset. Each day, training consisted of 90 tone/laser pairings and 10 interleaved tone-alone trials extended over four days of acquisition training. Following this acquisition training, mice were subjected to extinction training in which they were presented 100 tone-alone trials on each day. Within 2-3 days, acquisition training led to robust and statistically significant (one-way ANOVA, $F(2,8) = 4.403$, $p = 0.00168$) learned responses (LRs) evident as tone-evoked forelimb movements (Figures 3, S5 and S6, and Movie S3), which occurred in 83 ± 4.4% of trials and were rapidly extinguished over 3-4 days of extinction training (*post hoc* Tukey HSD, pairwise comparison to H4, E3 $p = 0.143$, E4 $p = 0.202$). Kinematic analyses showed that these learned movements involved the same limb and were similar in direction and temporal profile to those evoked by the laser pulses (Figure S5 and S6), but occurred earlier in time, as expected for predictive cerebellar learning (Medina, 2011; Ohyama et al., 2003). These findings indicate that synchronous PN depolarization can trigger the formation of associative motor memories allowing sensory stimuli to drive predictive forelimb movements.

Pairing PN inhibition with auditory tones also leads to associative learning

Evidence suggests that cerebellum-dependent associative learning involves circuit changes not only in the cerebellar cortex, but also in the cerebellar nuclei (Broussard and Kassardjian, 2004; Gao et al., 2012; Lisberger, 1994; Miles and Lisberger, 1981; Ohyama et

al., 2006; Raymond et al., 1996). In principle, pauses in PN activity driven by either complex spikes (Maiz et al., 2012a) or those developed in response to learning may instruct such changes by conveying transient periods of disinhibition to CNNs leading to the potentiation of tone-driven inputs to those CNNs. Mechanistically, NMDA receptor-dependent forms of long-term potentiation, which have been observed *in vitro*, could serve as the basis for this learning (Pugh and Raman, 2006). To test whether PN pauses are also sufficient to induce LRs we applied an associative training paradigm similar to that described above for ChR2, but using Arch to synchronously inhibit PNs. Pairing tones with Arch-driven PN pauses instructed tone-evoked forelimb movements (Figures 4, S5, and S6). LRs in Arch mice developed over several days of acquisition training and extinguished in response to tone-alone training (One-way ANOVA, $F(2,10) = 4.797$, $p = 0.0001$, *post hoc* Tukey HSD, in pairwise comparison to H4, E3 $p = 0.3234$); however, the percent of LRs was smaller than that observed for ChR2 and the individual LRs were of smaller amplitude (Table S1). These results indicate that disinhibition of CNNs alone is sufficient to drive associative motor learning, and suggest that synchronous pauses in the firing of groups of PNs can trigger circuit changes in the CNN that underlie associative learning.

PN inhibition-induced learning leads to mossy fiber sprouting in cerebellar nuclei

A recent study demonstrated that paired but not unpaired tone/air-puff training triggered significant structural changes in the cerebellar nuclei involving an increase in the number of mossy fiber endings related to the auditory tone (Boele et al., 2013). These findings support the hypothesis that associative conditioning leads to strengthening of specific mossy fiber to CNN connections, thereby contributing to LRs. We set out to examine whether similar structural plasticity occurs in the cerebellar nuclei of Arch trained animals. To first assess which areas of the cerebellar nuclei receive inputs from the PNs silenced by Arch activation during training, a small amount of dextran-conjugated Alexa 488 dye was injected into the forelimb motor region of lobulus simplex, the same site as we implanted our optical fibers (compare Figs. S1 and S7). Dye-filled axonal projections and terminals were found within discrete regions of the cerebellar nuclei, including large portions of the Anterior Interpositus Nucleus (IntA) and Dorsolateral Protuberance of the Medial Nucleus (MedDL) (Figure 5A), regions representing forelimb areas in rats (Pardoe and Apps, 2002). Next, we examined whether the number of mossy fiber terminals increased within these regions of the cerebellar nuclei after associative learning. To do this we divided sibling Arch cage-mates into two different groups — paired and unpaired. The paired group received 4 days of tone-laser paired training as described in Figure 4. The unpaired group was presented the same number of tone and laser stimuli over 4 days; however, these stimuli were presented in an unpaired, pseudorandomized fashion. To assess structural changes in mossy fiber inputs in the cerebellar nuclei, the number of mossy fiber puncta in the paired mice were compared against those in sibling matched unpaired mice (Figure 5B). The number of VGluT2-positive puncta was significantly higher in regions of the cerebellar nuclei receiving PN terminals originating from the forelimb area in paired vs unpaired mice (Figure 5C, MedDL: $p = 0.026$, $n = 4$ matched nuclear regions; IntA: $p = 0.024$, $n = 9$; IntP: $p = 0.0023$, $n = 7$; paired t-test, data from 3 or 4 matched pairs). In comparison, no significant changes in mossy fiber puncta were observed in the Lateral Nucleus (Lat, $p = 0.69$, $n = 5$; paired t-test, data from 3 matched pairs), consistent with the absence of dye-filled PN axons in this region

of the cerebellar nucleus (see methods). These results indicate that the LRs observed in Arch trained mice are accompanied by structural plasticity of mossy fiber inputs in the cerebellar nucleus similar to normal associative learning (Boele et al., 2013).

Learned movements trained with PN excitation versus inhibition show differences in timing

A critical aspect of associative motor memories is that they are adaptively timed, enabling predictive movements to be executed at precise times during sensory stimuli. Lesion studies suggest that these memories are stored in both the cerebellar cortex and nuclei but that information related to the timing of learned movements resides in the cerebellar cortex (Ohyama et al., 2006; Ohyama et al., 2003; Perrett et al., 1993). To compare the timing of learned movements generated by ChR2 versus Arch-training, we made kinematic measurements of LRs resulting from two different training intervals. For ChR2 trained animals, despite being similar in amplitude, the time courses of average, peak LRs were different, precisely anticipating the ends of the 250 or 500 ms training intervals (Figure 6A and Table S1). In contrast, LRs resulting from 250 and 500 ms training in Arch animals were similarly timed such that the LRs in mice trained with 500 ms intervals showed peak movement speed early in the stimulus (Figure 6B). Comparison between ChR2 and Arch of the latencies to peak-movement speeds for the 500 ms training intervals (Figure 6C) further support the conclusion that learned movements are significantly better timed in ChR2 trained animals.

The differences in timing of LRs described above suggest that learning resulting from PN inhibition occurs downstream within the cerebellar circuit, and a likely mechanism for this learning involves potentiation of tone-related mossy fiber inputs to CNNs (Boele et al., 2013; Miles and Lisberger, 1981; Ohyama et al., 2006; Raymond et al., 1996). Such a mechanism leads to the prediction that movements evoked by PN inhibition would be facilitated if accompanied by a sensory stimulus (e.g. tone) to which learning has occurred. We tested this prediction in Arch mice by comparing movements in response to the tone alone and to those evoked by the same tone plus a laser pulse timed to elicit PN pauses at the peak of the LR (Figure 7A). As shown in Figure 4, tone alone stimuli evoked no movement prior to learning. Following four days of paired training, inhibiting PNs using weak laser pulses facilitated tone-evoked LRs by 361 ± 63% (tone plus laser compared to tone-alone in interleaved trials, n = 3 mice, see Figure 7), leading to a significantly larger movement compared to the sum of movements evoked by laser stimulation and tone stimulation alone (sum = 202 ± 72%, $p < 0.005$, two-tailed, paired t-test). These results indicate that the contributions of PN pauses to movement are influenced by whether or not learning has occurred, and support the hypothesis that inhibition of PN firing can instruct memory-related changes in the cerebellar nuclei, a potential mechanistic substrate for “offline” consolidation from the cerebellar cortex to the cerebellar nuclei.

DISCUSSION

Here we combined optogenetics, high speed videography, and motion tracking to explore how modulation of the firing of groups of PNs in the simplex lobe acutely affect movement

and how coupling changes in PN firing with sensory experience can drive motor memory formation. This novel paradigm allows for the creation of artificial memories, powerfully demonstrating the generality of basic principles of cerebellar associative learning uncovered in classical eyeblink conditioning and vestibuloocular reflex plasticity. Our results also implicate critical functional roles for PN inhibition in the cerebellar circuit. On a fast time scale, reductions in PN activity lead to movement while on a longer time scale, reductions in PN activity lead to behavioral learning, likely by stimulating increases in mossy fiber input to CNNs. Finally, by engaging distinct circuit elements with ChR2 and Arch training, we show that learned forelimb movements exhibit different timing profiles, providing support for the hypothesis that cerebellar learning results from circuit modifications in both the cerebellar cortex and nucleus with plasticity in the cerebellar cortex required for precisely timed learned movements.

Synchronous reductions in PN firing drive forelimb movements

Despite extensive study, direct links between PN activity and specific aspects of movement have been unclear. While electrical microstimulation of the cerebellar nuclei reliably triggers limb movements (Ekerot et al., 1995; Rispal-Padel et al., 1981, 1982; Schultz et al., 1976, 1979) and microstimulation of floccular and vermal regions of cerebellar cortex leads to movements of the head, parts of the face, or eyes (Cohen et al., 1965; De Zeeuw and Koekkoek, 1997; Esakov and Pronichev, 2001; Lisberger, 1994; Noda and Fujikado, 1987; Ron and Robinson, 1973), there are no reports in the literature of limb movements evoked by electrical stimulation of the cerebellar cortex. Interestingly, microstimulation in more lateral areas of cerebellar cortex located near those under study here has been reported to suppress learned eyeblink movements (Hesslow, 1994).

Given the well-established correlation between reductions in PN firing and learned movements, the issue of how PN firing contributes to movement is critical (De Zeeuw et al., 2011; Jirenhed et al., 2007; Lisberger et al., 1994a; Medina and Lisberger, 2008). Our findings comparing the effects of stimulating ChR2 and Arch in PNs indicate that synchronous pauses in spontaneous firing of PNs in the simplex lobe are sufficient to elicit rapid forelimb movements (Figures 1 and 2). These results are in line with recent reports showing facial movements in response to ChR2-elicited synaptic inhibition of PNs (Heiney et al., 2014) and delayed postural movements elicited by ChR2 stimulation of PNs (Witter et al., 2013). Taken together the findings imply that populations of functionally related PNs promote movement by synchronizing the inter-spike intervals on a fast time scale thereby disinhibiting CNNs to drive movements (Person and Raman, 2012).

Modulation of PN activity in conjunction with sensory stimuli induces motor memories

We also show that specific PN activity patterns, when paired with sensory stimuli, can drive robust, associative motor learning (Figures 3 and 4). The resulting learned movements closely resemble the acutely evoked movements recorded in our study, consistent with the somatotopic map known to exist in cerebellum (Apps and Hawkes, 2009). The ChR2-induced, artificial memories described here also have a number of properties similar to natural forms of cerebellar learning such as eyeblink conditioning and vestibuloocular reflex plasticity (Raymond et al., 1996). These include the rate at which learning and extinction

occur, the predictive timing of LRs, the registration between training interval and learned movement timing, and the structural plasticity observed in the nucleus. The findings suggest a conserved mechanism by which cerebellar circuits can make use of sensorimotor information to prompt adaptive movements, at least within the intermediate cerebellum.

The learning in response to Arch stimulation demonstrates that PN inhibition can trigger the formation of associative motor memories. A likely mechanism for this learning involves disinhibition of CNNs leading to an enhancement in the strength of mossy fiber collateral inputs to CNNs. In support of this model, brain slice studies have identified an NMDA receptor-dependent form of long term potentiation of excitatory inputs to CNNs that is triggered upon release of hyperpolarization (Pugh and Raman, 2006). Our findings indicate that training results in increases in presumed mossy fiber innervation of areas within the cerebellar nuclei targeted by modulated PNs (Figure 5), consistent with a strengthening of tone-related mossy fiber inputs. The results demonstrate that release from hyperpolarization caused by the simultaneous pause in firing of a population of PNs can serve as the teaching signal driving such plasticity.

Ensuring precise timing of movements is a hallmark of cerebellar function, as demonstrated for classically conditioned eyeblinks (Ohyama and Mauk, 2001; Ohyama et al., 2006; Perrett et al., 1993). Pharmacological inactivation of the cerebellar cortex after eyeblink training does not abolish LRs but leads to rapid eyeblinks with time courses that are no longer in register with the training interval. The Arch-induced learning described here shows a similar profile (Figure 6), consistent with learning under these circumstances being confined to the cerebellar nucleus (McCormick and Thompson, 1984).

A unifying hypothesis accounting for optogenetic and normal forms of learning is presented in Figure 8. We posit that pairing ChR2 excitation of PNs with sensory stimuli triggers changes in synapses encoding those sensory stimuli at PNs and CNNs, leading to sensory-evoked pauses in PNs and bursts in CNNs, and robust, well-timed learned movements. In contrast, pairing Arch stimulation with sensory stimuli leads only to changes in inputs to CNNs (compare Figures 8B and 8C). We hypothesize that less robust and less well-timed motor learned movements in Arch trained mice occur because sensory-evoked CNN bursts do not occur coincidently with PN disinhibition (Figure 8C). Supporting this interpretation, we demonstrate that in Arch trained mice, imposition of pauses in upstream PNs (Figure 8D) facilitates movements elicited by the sensory conditioning stimulus (Figure 7). Taken together, these results provide further evidence that cerebellar mediated learning recruits plastic changes at multiple sites within the circuit.

Functional implications

By generating artificial motor memories through optogenetic training, we show that the effects of PN pauses on movement are augmented by learning, providing support for models of cerebellar learning that hypothesize learning-related circuit changes in the cerebellar nucleus (Miles and Lisberger, 1981; Perrett et al., 1993). Our results further show that disinhibition of CNNs is sufficient to drive associative memory formation. The fact that PN pauses can instruct memory formation provides proof of concept support for theories of cerebellar memory formation that propose that learning-related changes in the cerebellar

cortex precede, and may be necessary for, structural plasticity and consolidation in the cerebellar nucleus (Cooke et al., 2004; Kassardjian et al., 2005; Ohyama et al., 2006).

EXPERIMENTAL PROCEDURES

Animals

All animal procedures were performed in accordance with National Institutes of Health standards and were approved by the University of California, Los Angeles Institutional Animal Care and Use Committee. Male and female mice homozygous for L7-Cre (B6.129-Tg(Pcp2-cre)2Mpin/J, Jackson Labs) were crossed with either an animal homozygous for ChR2-eYFP (Ai32, B6;129S-*Gt(ROSA)26Sor*$^{tm32(CAG-COP4*H134R/EYFP)Hze}$/J, Jackson Labs) or Arch-eGFP (Ai35, B6;129S-*Gt(ROSA)26Sor*$^{tm35.1(CAG-aop3/GFP)Hze}$*/J*, Jackson Labs*)*. Subsets of animals at the end of behavioral experiments were perfused (4% paraformaldehyde) and their brains removed. Fluorescent images of the whole cerebellum were obtained at 14× using a Zeiss (Stereo Discovery V12) dissecting microscope and camera (Axiocam MRm) in order to examine and document the sites of chronic fiber placement in each mouse (Figure S1).

In vitro electrophysiology

Adult mice 23-34g (L7-Cre/Arch or ChR2) in weight were anaesthetized and decapitated. Parasagittal cerebellar slices (300 μm) were cut in an ice cold (4°C), low-sodium cutting solution using a vibratome (Leica VT-1000). Slices were incubated for ~30 min. at 35°C and allowed to sit at room temperature before electrophysiological recordings at ~34°C. Cutting and recording media were bubbled with 95% O_2 and 5% CO_2. The low-sodium cutting solution consisted of (in mM): 82.7 NaCl, 2.4 KCl, 1.4 NaH_2PO_4, 0.5 $CaCl_2$, 6.8 $MgCl_2$, 23.8 $NaHCO_3$, 65 sucrose, 23.7 dextrose and the recording solution consisted of (in mM): 119 NaCl, 2.5 KCl, 1.25 NaH_2PO_4, 2 $CaCl_2$, 1 $MgCl_2$, 26 $NaHCO_3$, 25 dextrose.

Cells were visualized using an upright microscope (Zeiss Axioskop II) with a 40X water immersion lens using infrared differential interference contrast microscopy. Optical activation of ChR2 or Arch was achieved using an LED light source (532 nM, THOR labs) projected through the epifluorescence pathway of the microscope. Pulses of light were either triggered directly by TTL signals from pClamp to the LED controller or through a signal generator (Master 8, AMPI) triggered by pClamp. For all graphs, optical stimulation was elicited at t = 0 ms. Data was acquired using pClamp9 (Molecular Devices) at 50 kHz for intracellular recordings and 5-10 kHz for extracellular recordings. A Multiclamp 700B was used to record electrophysiological signals. In voltage clamp, the pipette and cellular capacitance (≥ 80%) were compensated for using onboard circuitry. The pipette solution for PN voltage and current clamp recordings contained (in mM): 126 $KMSO_3$, 10 KCl, 4 NaCl, 10 HEPES, 0.5 EGTA, 14 Tris-phosphocreatine, 2 MgATP, 0.4 NaGTP. Experiments were analyzed using custom macros written for Igor Pro (Taro Tools, Dr. Taro Ishikawa, https://sites.google.com/site/tarotoolsregister/).

Surgical procedures

All surgical procedures were performed under isoflurane (1%) anesthesia, and performed at least 2 days prior to either *in vivo* electrophysiological recording or behavioral manipulation. Animals were placed into a stereotaxic device and custom made head-bars (FabtoOrder) were glued to the skull using Vetbond (3M) and dental cement (Bosworth Co.). For *in vivo* electrophysiological recordings large craniotomies were made over the medial or left cerebellum. The exposed site was then filled over with a silicon based elastomer (Kwik-cast, WPI) that was easily removed just prior to recording. For behavioral experiments, chronically implanted optic fiber cannulas (Doric lenses), dipped in DiI (Sigma), were stereotaxically positioned (RC:6.25mm, ML:1.9mm, DV:2mm) into the brain through small craniotomies, and fixed into place using Meta-Bond (Parkell). Whole mount fluorescence visualization (see Figure S1) allowed *posthoc* localization of the fiber.

In vivo electrophysiology

Head-fixed animals were allowed to move in place freely on a spinning disk (Ware Flying Saucer). Optrodes constructed of fiber optic cannulas (Doric lenses) glued ~400 μm behind 1-5 MΩ Parylene-C insulated tungsten electrodes (A-M Systems) were inserted into craniotomies and vertically driven into the cerebellum using a micromanipulator (Sutter). Electrical signals were recorded with an Axopatch 200B amplifier (V-clamp mode) and data acquired in pClamp9 (50 kHz). A TTL controlled, 100 W diode pumped solid state laser (532 nm, Opto-Engine) was coupled through a patch cable (Doric Lenses) to the optrode to deliver brief pulses of light. Spike detection and data analysis were performed in Igor Pro 6 using custom macros (adapted from Tarotools).

Behavior

All animals were habituated to the behavioral setup for at least 4 days prior to training. Animals were head-fixed but allowed to move freely on a spinning disk (Ware, Inc.). A TTL controlled 100 W, 532 nm diode laser (CNI Laser, Optoengine), launched into a patch cable and connected to the fiber optic cannula were used to activate either ChR2 or Arch within the forelimb region of the cerebellum for the indicated durations determined by TTL control. Power output per unit area, measured regularly from a pristine fiber segment identical to that implanted, ranged from 320 to 1910 mW/mm^2. These values are calculated by dividing total power (10-60 mW) by the cross sectional area of the 200 μm diameter optical fiber used in our study. The values used here compare well to values of 142 to 16,000 mW/mm^2 reported by Heiney et al (2014) for the 20-30 μm diameter fibers used in their study.

Optical stimulation was paired with a tone coordinated using custom routines written in LabView and controlled via TTL pulses from a NIDAQ board (National Instruments). Epochs of high speed video (200 f/s) were also synchronized via TTL and obtained with a Giga-E camera (Allied). Kinematic measurements were made offline using Custom LabView routines that allowed for the tracking of an IR reflective button (Mocap solutions) adhered to the mouse's wrist. Data were further analyzed using custom macros in Igor Pro 6 allowing infrequent tracking artifacts to be excised. A subset of the kinematic data were also analysed by MTrackJ in ImageJ and the results were identical to the automated LabView

routine. All speed-vs-time traces were smoothed by a binomial function with a factor of 3. All error bars or shaded errors in figures represent s.e.m.

Custom Igor procedures were used to automatically sort individual trials for rejection or analysis. Rejected trials included those in which movement speed exceeded 0.04 m/s during a 500 ms epoch prior to tone onset (baseline period) or trials in which movement speed exceeded 0.04 m/s within 50 ms after tone onset (startle period). On average this resulted in variable rejection rates of 35-70 trials per mouse per day. In trials with tone and laser stimuli, LRs were judged to occur when movement speed exceeded 0.04 m/s in the time epoch from 50 ms after tone onset until laser onset; in tone alone trials LRs could occur from 50 ms following tone onset until tone offset which co-terminated with the laser pulse offset. To determine percent LR, the number of LR trials was divided by total number of analyzed trials (excluding rejected trials). We chose the term “learned response” rather than the more conventionally used term “conditioned response” to reflect the fact that LRs in this study are generated by optogenetic stimuli rather than by behavioral error signals, and because LRs in ChR2- and Arch-trained animals are likely to result from distinct circuit mechanisms.

PN tract tracing

Dextran-conjugated Alexa 488 (210 nL, 5 mM) was stereotaxically injected into the cerebellar cortex of wild-type mice at the same coordinates used for fiber implants. After allowing retrograde transport of the dye for 7 days, mice were anesthetized (Pentobarbital) and then perfused with a 4% paraformaldehyde phosphate buffered saline (freshly diluted from 32% stock, Electron Microscopy Sciences). Brains were subsequently removed and incubated in a phosphate buffered solution containing 30% sucrose for up to 2 days. Brains were then embedded in optimal cutting temperature solution (Tissue-Tech) at −80°C. Sections, cut in a cryostat at 60 μm, were immunostained using mouse α-NeuN monoclonal antibody (1:500, Millipore) and goat α-mouse Alexa 568 secondary antibody (1:300, Life Technologies). Confocal images were obtained at 10× and 20× (Zeiss, 0.3 and 0.8 NA, respectively) using a Zeiss 710 laser-scanning confocal microscope. Raw images were processed and analyzed using ImageJ (NIH). Quantification of dye filled axons was performed by first thresholding images of sagittal or coronal cerebellar sections and then calculating the percent immunofluorescence in each nucleus (Lat = 0.013 ± 0.007 %, n = 7 sections; IntA = 20.5 ± 5.93 %, n = 17; IntP = 6.87 ± 1.85 %, n = 17; MedDL = 38.8 ± 5.38 %, n = 17; Med = 4.81 ± 1.45 %, n = 16; data from 2 animals). Each section was also visually examined for the presence of dye-filled PN axons (Lat = 0/12 sections, IntA = 12/12, IntP = 13/17, MedDL = 16/16, Med = 14/17; n = 2 animals). Any labelled tubular structure with thicknesses of more than 3 μm were presumed to be endothelial cells composing blood vessels which were found throughout the sections and thus excluded from analysis (see Fig. S7).

Learning-induced structural plasticity in the cerebellar nuclei

L7-Arch mice were habituated on the behavioral platform for at least 4 days. Cage siblings were split into paired (100 pairs of 250 ms 2 kHz tone coterminating with 75 ms laser stimulation, randomized intertrial interval between 20 and 40 s) and unpaired (100 tone

alone/laser alone trials, randomized intertrial interval between 10 and 20 s) training groups. For the unpaired training, tone and laser presentation was performed in a pseudorandomized order. After training for 4 consecutive days, the mice were perfused with 4% paraformaldehyde and prepared for cryosectioning as described above. Parasagittal sections (30 μm) were then cut and stained with mouse α-VGluT2 monoclonal antibody (1:300, Millipore) and goat α-mouse Alexa 568 secondary antibody (1:300). Images of the cerebellum were first obtained using a Zeiss 710 confocal microscope with a 10× objective to identify the cerebellar nuclei. Each identified region of the cerebellar nuclei was then captured as continuous stacks of confocal images (0.64 μm thick) using a 63× objective (Zeiss, 1.4 NA) and custom acquisition software (Zeiss). After image acquisition, every 5th image in the z-stack was isolated to prevent recounting the same puncta. The VGluT2+ puncta were quantified by first thresholding the image to isolate immunopositive signals. The particle count tool in ImageJ (NIH) was then used to count discrete puncta in each identified cerebellar nuclei.

Supplementary Material

Refer to Web version on PubMed Central for supplementary material.

ACKNOWLEDGEMENTS

We would like to thank Dr. Jaione Maiz for pilot experiments, Ms. Tracy Lin for help with behavioral training and histology, Dr. Matthew Shtrahman for technical support, and other members of the Otis laboratory for comments on the manuscript. We also thank the laboratories of Drs. Carolyn Houser, Ben Novitch, and Larry Hoffman for access to equipment used for histological processing and analysis. We thank Dr. Larry Hoffman for helpful comments on histological analyses. This research was supported by NIH grants R01 NS068408, R56 NS033123, and S10RR029267 and a McKnight Foundation Award to T.S.O. P.J.M. received support from F32 NS074719 and both P.J.M. and A.M.B.R. received support from T32 NS058280.

REFERENCES

Albus JS. A Theory of Cerebellar Function. Mathematical Biosciences. 1971; 10:25–61.

Apps R, Hawkes R. Cerebellar cortical organization: a one-map hypothesis. Nat Rev Neurosci. 2009; 10:670–681. [PubMed: 19693030]

Boele HJ, Koekkoek SK, De Zeeuw CI, Ruigrok TJ. Axonal sprouting and formation of terminals in the adult cerebellum during associative motor learning. J Neurosci. 2013; 33:17897–17907. [PubMed: 24198378]

Broussard DM, Kassardjian CD. Learning in a simple motor system. Learn Mem. 2004; 11:127–136. [PubMed: 15054127]

Cao Y, Maran SK, Dhamala M, Jaeger D, Heck DH. Behavior-related pauses in simple-spike activity of mouse Purkinje cells are linked to spike rate modulation. J Neurosci. 2012; 32:8678–8685. [PubMed: 22723707]

Catz N, Dicke PW, Thier P. Cerebellar-dependent motor learning is based on pruning a Purkinje cell population response. Proc Natl Acad Sci U S A. 2008; 105:7309–7314. [PubMed: 18477700]

Chettih SN, McDougle SD, Ruffolo LI, Medina JF. Adaptive timing of motor output in the mouse: the role of movement oscillations in eyelid conditioning. Front Integr Neurosci. 2011; 5:72. [PubMed: 22144951]

Cohen B, Goto K, Shanzer S, Weiss AH. Eye movements induced by electric stimulation of the cerebellum in the alert cat. Exp Neurol. 1965; 13:145–162. [PubMed: 5320100]

Cooke SF, Attwell PJ, Yeo CH. Temporal properties of cerebellar-dependent memory consolidation. J Neurosci. 2004; 24:2934–2941. [PubMed: 15044532]

De Zeeuw CI, Hoebeek FE, Bosman LW, Schonewille M, Witter L, Koekkoek SK. Spatiotemporal firing patterns in the cerebellum. Nat Rev Neurosci. 2011; 12:327–344. [PubMed: 21544091]

De Zeeuw CI, Koekkoek SK. Signal processing in the C2 module of the flocculus and its role in head movement control. Prog Brain Res. 1997; 114:299–320. [PubMed: 9193151]

Ekerot CF, Jorntell H, Garwicz M. Functional relation between corticonuclear input and movements evoked on microstimulation in cerebellar nucleus interpositus anterior in the cat. Exp Brain Res. 1995; 106:365–376. [PubMed: 8983981]

Esakov SA, Pronichev IV. Motor representations of facial muscles and vibrissae in the cerebellar cortex of the white mouse *Mus musculus*. J Evol Biochem Physiol. 2001; 37:642–647.

Gao Z, van Beugen BJ, De Zeeuw CI. Distributed synergistic plasticity and cerebellar learning. Nat Rev Neurosci. 2012; 13:619–635. [PubMed: 22895474]

Greger B, Norris SA, Thach WT. Spike firing in the lateral cerebellar cortex correlated with movement and motor parameters irrespective of the effector limb. J Neurophysiol. 2004; 91:576–582. [PubMed: 12878717]

Heck DH, De Zeeuw CI, Jaeger D, Khodakhah K, Person AL. The neuronal code(s) of the cerebellum. J Neurosci. 2013; 33:17603–17609. [PubMed: 24198351]

Heiney SA, Kim J, Augustine GJ, Medina JF. Precise control of movement kinematics by optogenetic inhibition of Purkinje cell activity. J Neurosci. 2014; 34:2321–2330. [PubMed: 24501371]

Hesslow G. Inhibition of classically conditioned eyeblink responses by stimulation of the cerebellar cortex in the decerebrate cat. J Physiol. 1994; 476:245–256. [PubMed: 8046641]

Hesslow G, Ivarsson M. Suppression of cerebellar Purkinje cells during conditioned responses in ferrets. Neuroreport. 1994; 5:649–652. [PubMed: 8025262]

Ito, M. The Cerebellum and Neural Control. Raven; San Diego: 1984.

Jirenhed DA, Bengtsson F, Hesslow G. Acquisition, extinction, and reacquisition of a cerebellar cortical memory trace. J Neurosci. 2007; 27:2493–2502. [PubMed: 17344387]

Kassardjian CD, Tan YF, Chung JY, Heskin R, Peterson MJ, Broussard DM. The site of a motor memory shifts with consolidation. J Neurosci. 2005; 25:7979–7985. [PubMed: 16135754]

Ke MC, Guo CC, Raymond JL. Elimination of climbing fiber instructive signals during motor learning. Nat Neurosci. 2009; 12:1171–1179. [PubMed: 19684593]

Kojima Y, Soetedjo R, Fuchs AF. Changes in simple spike activity of some Purkinje cells in the oculomotor vermis during saccade adaptation are appropriate to participate in motor learning. J Neurosci. 2010; 30:3715–3727. [PubMed: 20220005]

Lisberger SG. Neural basis for motor learning in the vestibuloocular reflex of primates. III. Computational and behavioral analysis of the sites of learning. J Neurophysiol. 1994; 72:974–998. [PubMed: 7983549]

Lisberger SG, Pavelko TA, Bronte-Stewart HM, Stone LS. Neural basis for motor learning in the vestibuloocular reflex of primates. II. Changes in the responses of horizontal gaze velocity Purkinje cells in the cerebellar flocculus and ventral paraflocculus. J Neurophysiol. 1994a; 72:954–973. [PubMed: 7983548]

Lisberger SG, Pavelko TA, Broussard DM. Neural basis for motor learning in the vestibuloocular reflex of primates. I. Changes in the responses of brain stem neurons. J Neurophysiol. 1994b; 72:928–953. [PubMed: 7983547]

Maiz J, Karakossian MH, Pakaprot N, Robleto K, Thompson RF, Otis TS. Prolonging the postcomplex spike pause speeds eyeblink conditioning. Proc Natl Acad Sci U S A. 2012; 109:16726–16730. [PubMed: 22988089]

Marr D. A theory of cerebellar cortex. J Physiol. 1969; 202:437–470. [PubMed: 5784296]

Mauk MD. Roles of cerebellar cortex and nuclei in motor learning: contradictions or clues? Neuron. 1997; 18:343–346. [PubMed: 9115728]

Mauk MD, Donegan NH. A model of Pavlovian eyelid conditioning based on the synaptic organization of the cerebellum. Learning & memory. 1997; 4:130–158. [PubMed: 10456059]

McCormick DA, Thompson RF. Cerebellum: essential involvement in the classically conditioned eyelid response. Science. 1984; 4633:296–299. [PubMed: 6701513]

Medina JF. The multiple roles of Purkinje cells in sensori-motor calibration: to predict, teach and command. Curr Opin Neurobiol. 2011; 21:616–622. [PubMed: 21684147]

Medina JF, Lisberger SG. Links from complex spikes to local plasticity and motor learning in the cerebellum of awake-behaving monkeys. Nat Neurosci. 2008; 11:1185–1192. [PubMed: 18806784]

Miles FA, Lisberger SG. Plasticity in the vestibulo-ocular reflex: a new hypothesis. Annu Rev Neurosci. 1981; 4:273–299. [PubMed: 6784658]

Noda H, Fujikado T. Involvement of Purkinje cells in evoking saccadic eye movements by microstimulation of the posterior cerebellar vermis of monkeys. J Neurophysiol. 1987; 57:1247–1261. [PubMed: 3585467]

Ohyama T, Mauk M. Latent acquisition of timed responses in cerebellar cortex. J Neurosci. 2001; 21:682–690. [PubMed: 11160447]

Ohyama T, Nores WL, Medina JF, Riusech FA, Mauk MD. Learning-induced plasticity in deep cerebellar nucleus. J Neurosci. 2006; 26:12656–12663. [PubMed: 17151268]

Ohyama T, Nores WL, Murphy M, Mauk MD. What the cerebellum computes. Trends Neurosci. 2003; 26:222–227. [PubMed: 12689774]

Okamoto T, Shirao T, Shutoh F, Suzuki T, Nagao S. Post-training cerebellar cortical activity plays an important role for consolidation of memory of cerebellum-dependent motor learning. Neurosci Lett. 2011; 504:53–56. [PubMed: 21911037]

Otis TS, Mathews PJ, Lee KH, Maiz J. How do climbing fibers teach? Front Neural Circuits. 2012; 6:95. [PubMed: 23226116]

Pardoe J, Apps R. Structure-function relations of two somatotopically corresponding regions of the rat cerebellar cortex: olivo-cortico-nuclear connections. Cerebellum. 2002; 1:165–184. [PubMed: 12879979]

Perrett SP, Ruiz BP, Mauk MD. Cerebellar cortex lesions disrupt learning-dependent timing of conditioned eyelid responses. J Neurosci. 1993; 13:1708–1718. [PubMed: 8463846]

Person AL, Raman IM. Purkinje neuron synchrony elicits time-locked spiking in the cerebellar nuclei. Nature. 2012; 481:502–505. [PubMed: 22198670]

Popa LS, Hewitt AL, Ebner TJ. Purkinje Cell Simple Spike Discharge Encodes Error Signals Consistent with a Forward Internal Model. Cerebellum. 2013

Pugh JR, Raman IM. Potentiation of mossy fiber EPSCs in the cerebellar nuclei by NMDA receptor activation followed by postinhibitory rebound current. Neuron. 2006; 51:113–123. [PubMed: 16815336]

Raymond JL, Lisberger SG, Mauk MD. The cerebellum: a neuronal learning machine? Science. 1996; 272:1126–1131. [PubMed: 8638157]

Rispal-Padel L, Cicirata F, Pons C. Contribution of the dentato-thalamo-cortical system to control of motor synergy. Neurosci Lett. 1981; 22:137–144. [PubMed: 7231805]

Rispal-Padel L, Cicirata F, Pons C. Cerebellar nuclear topography of simple and synergistic movements in the alert baboon (Papio papio). Exp Brain Res. 1982; 47:365–380. [PubMed: 6889975]

Ron S, Robinson DA. Eye movements evoked by cerebellar stimulation in the alert monkey. J Neurophysiol. 1973; 36:1004–1022. [PubMed: 4202613]

Schonewille M, Gao Z, Boele HJ, Veloz MF, Amerika WE, Simek AA, De Jeu MT, Steinberg JP, Takamiya K, Hoebeek FE, et al. Reevaluating the role of LTD in cerebellar motor learning. Neuron. 2011; 70:43–50. [PubMed: 21482355]

Schultz W, Montgomery EB Jr. Marini R. Stereotyped flexion of forelimb and hindlimb to microstimulation of dentate nucleus in cebus monkeys. Brain Res. 1976; 107:151–151. [PubMed: 817785]

Schultz W, Montgomery EB Jr. Marini R. Proximal limb movements in response to microstimulation of primate dentate and interpositus nuclei mediated by brain-stem structures. Brain. 1979; 102:127–146. [PubMed: 106923]

Shutoh F, Ohki M, Kitazawa H, Itohara S, Nagao S. Memory trace of motor learning shifts transsynaptically from cerebellar cortex to nuclei for consolidation. Neuroscience. 2006; 139:767–777. [PubMed: 16458438]

Titley HK, Heskin-Sweezie R, Chung JY, Kassardjian CD, Razik F, Broussard DM. Rapid consolidation of motor memory in the vestibuloocular reflex. J Neurophysiol. 2007; 98:3809–3812. [PubMed: 17977924]

Witter L, Canto CB, Hoogland TM, de Gruijl JR, De Zeeuw CI. Strength and timing of motor responses mediated by rebound firing in the cerebellar nuclei after Purkinje cell activation. Front Neural Circuits. 2013; 7:133. [PubMed: 23970855]

Wulff P, Schonewille M, Renzi M, Viltono L, Sassoe-Pognetto M, Badura A, Gao Z, Hoebeek FE, van Dorp S, Wisden W, et al. Synaptic inhibition of Purkinje cells mediates consolidation of vestibulo-cerebellar motor learning. Nature neuroscience. 2009; 12:1042–1049.

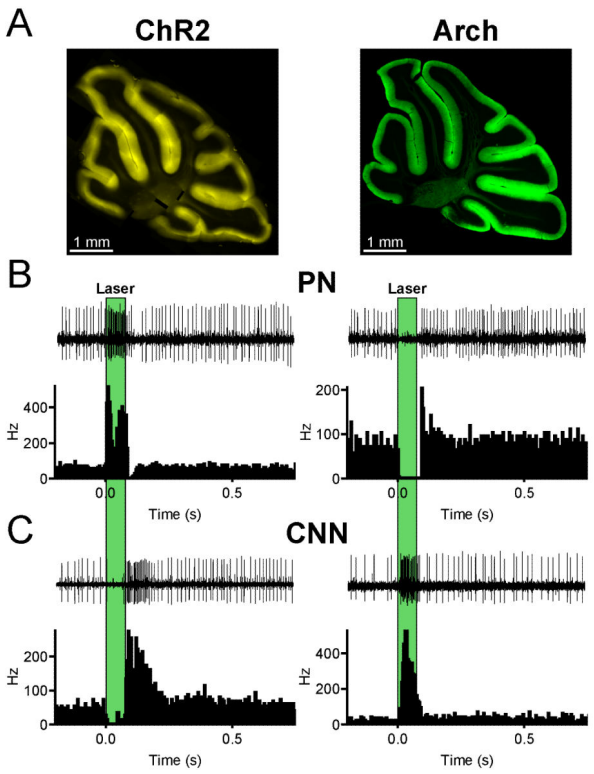

Figure 1. Pauses in PN firing drive motor output

(A) Photomicrographs of parasagittal cerebellar sections showing expression of ChR2-eYFP (left) and Arch-GFP (right) selectively in PNs. (B) *In vivo*, single unit optrode recordings from PNs in response to 75 ms light activation of ChR2 (left) or Arch (right) in awake mice. Laser pulse duration is indicated by green boxes. Single extracellular traces are shown above the peri-stimulus time histograms for each cell. (C) *In vivo* recordings from CNNs in ChR2 (left) and Arch (right) mice in response to 75 ms light pulses delivered to PN axons in the cerebellar nucleus. See also Figures S2 and S3.

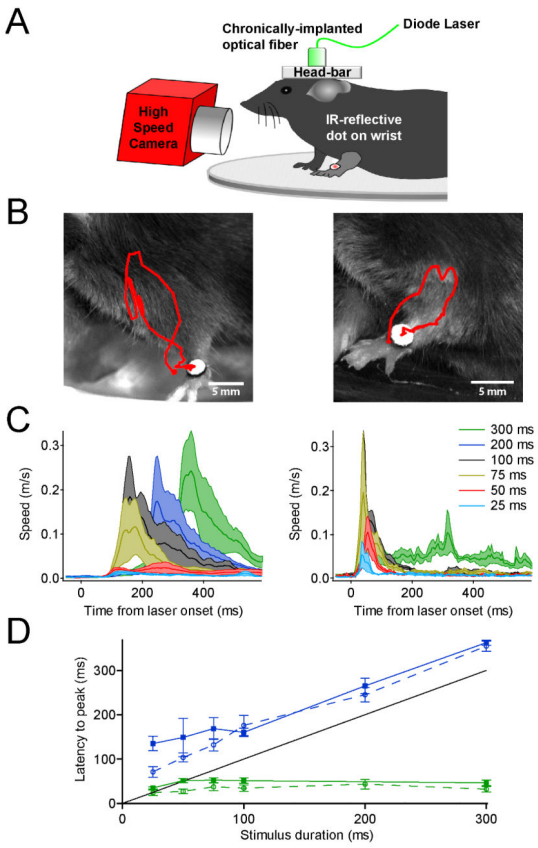

Figure 2. Optogenetically elicited, rapid forelimb movements

(A) Illustration of head-fixed animal preparation used for behavioral studies. A high-speed video camera coupled with infrared (IR) illumination allowed movement of the wrist, tagged with an IR-reflective dot, to be tracked offline using motion tracking software. (B) Shown is a single frame taken from the end of a video in which a 100 ms laser pulse was delivered through a chronically implanted fiber optic in the forelimb region of the ipsilateral cerebellar cortex. The resulting ChR2 (left) and Arch (right) forelimb trajectories are traced in red. (C) Mean forelimb speed versus time relative to the onset of laser pulses of the indicated durations. Note that in ChR2 mice (left) movement onset is time-locked to the end of laser illumination while in Arch mice (right) movement occurs independently of pulse duration with a fixed delay following illumination onset. (D) Delay to peak movement speed (solid lines) and peak CNN firing frequency (dotted lines) are plotted together as a function of laser pulse duration. Data are plotted for ChR2 (blue, n = 7) and Arch (green, n=9) mice. Note that in ChR2 mice movement and peak firing occur with a fixed delay from the end of the laser pulses (indicated by black line), whereas in Arch mice movement and peak CNN firing occur at a fixed delay from pulse onset. See also Figures S2, S3, and Movies S1 and S2.

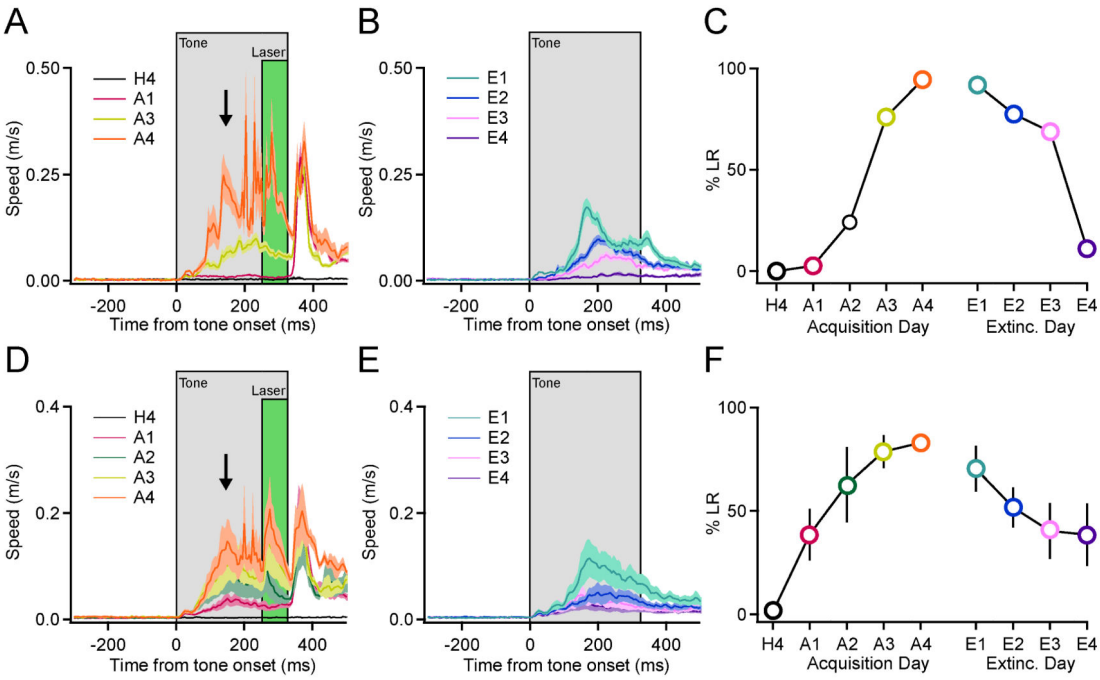

Figure 3. Pairing ChR2 activation in PNs with auditory tones leads to predictive, tone-evoked forelimb movements

(A) Mean speed (± s.e.m. indicated by lighter shading) of forelimb movement for a single animal across all trials on indicated days of training (H4, habituation day 4; A1, 3, and 4, acquisition training days 1, 3 and 4). All analyzed trials are included. The timing of the tone (325 ms) and laser (75 ms) pulses are indicated with grey and green boxes, respectively, and the arrow indicates the LR. Note the gradual appearance of tone-evoked movement with acquisition training and abolishment of this movement with extinction training. (B) Mean movement speed during extinction training (E1 to 4 = extinction day 1 to 4) for the same animal. (C) Summary plot for this animal indicating percent LR across acquisition and extinction training. Colored symbols correspond to mean speed versus time traces in A and B. (D, E) Mean speed profiles during acquisition (D), and extinction (E), n = 4 mice for each. Lighter shading indicates s.e.m. across animals. (F) Summary of percent LR ± s.e.m. (n = 4 mice) across days. See also Figures S5, S6, and Movie S3

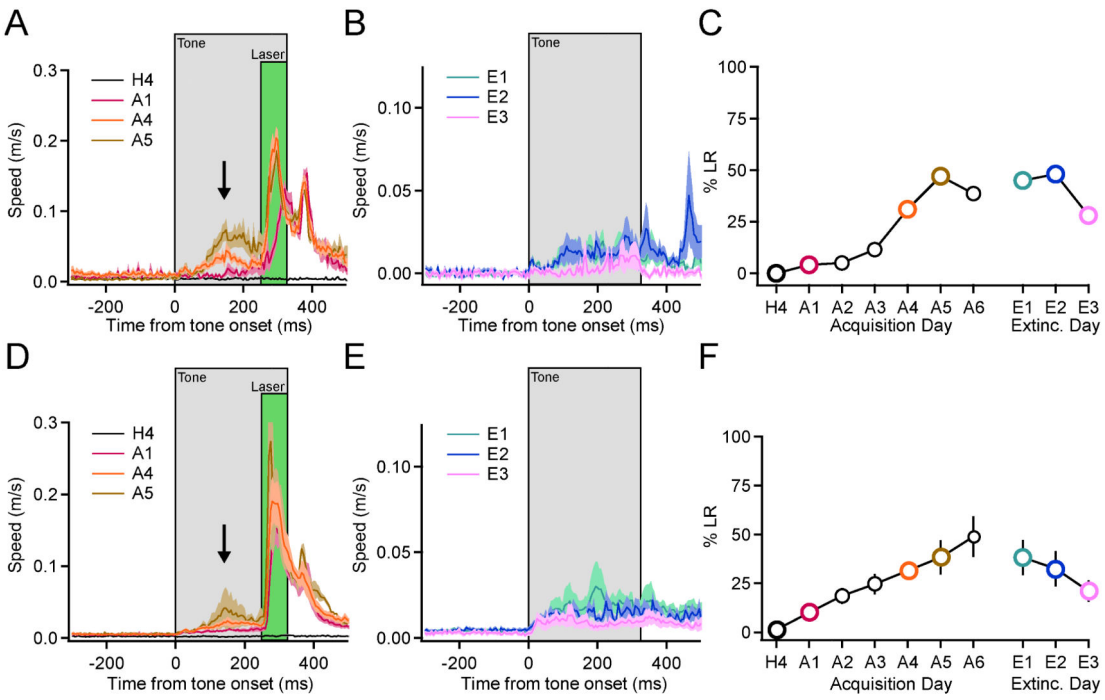

Figure 4. Pairing Arch activation in PNs with auditory tones leads to predictive, tone-evoked forelimb movements

(A) Mean speed (± s.e.m. indicated by lighter shading) of forelimb movement for a single animal across all trials on indicated days of training (H4, habituation day 4; A1, 4, and 5, acquisition training days 1, 4 and 5). All analyzed trials are included. The timing of the tone (325 ms) and laser (75 ms) pulses are indicated with grey and green boxes, respectively, and the arrow indicates the LR. Note the gradual appearance of tone-evoked movement with acquisition training and abolition of this movement with extinction training. (B) Mean speed during extinction training (E1 to 3 = extinction day 1 to 3) for the same animal. (C) Summary plot for this animal indicating percent LR across acquisition and extinction training. Colored symbols correspond to mean speed versus time traces in A and B. (D, E) Average speed profiles for Arch mice during acquisition (D, n = 6 mice), and extinction (E, n = 3 mice). Lighter shading indicates s.e.m. across animals. (F) Summary of percent LR ± s.e.m. (n = 2-6 mice) across days. See also Figures S5, S6, and Movie S4.

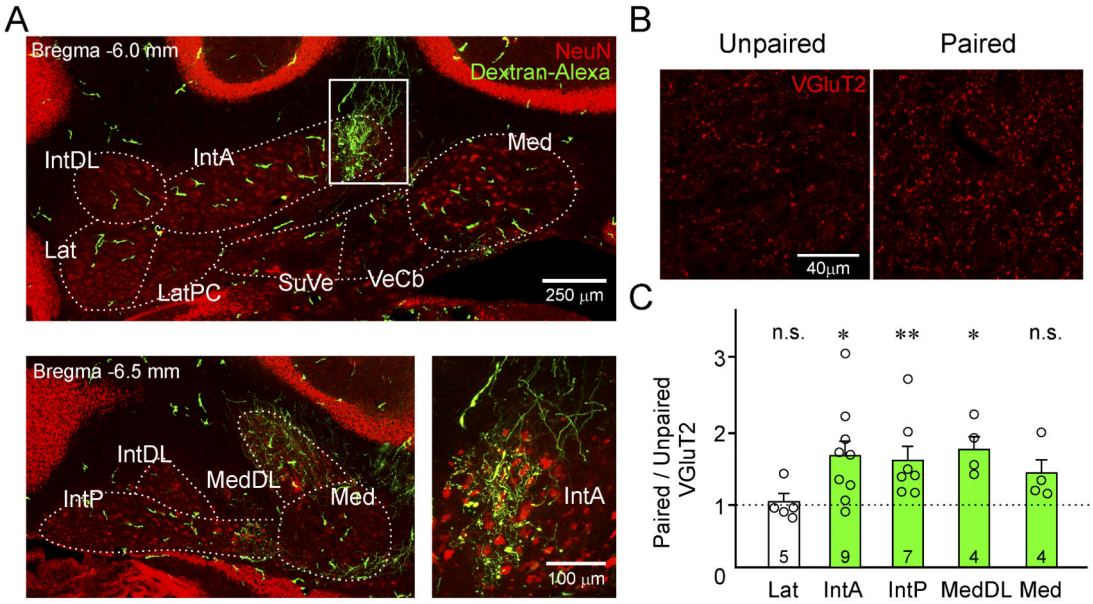

Figure 5. Associative motor learning induces formation of VGluT2+ terminals in a subset of cerebellar nuclei in L7-Arch mice

(A) Coronal sections, counterstained with the neuronal marker, NeuN (red), show dextran-conjugated Alexa 488 filled PN axons (thin green lines) that originate from the same site as our optic fiber placements. Dye-filled PN axons are apparent within the Anterior Interpositus (IntA), Posterior Interpositus (IntP), Medial (Med), and Dorsolateral Protuberance of the Medial nucleus (MedDL). Green objects of large diameter are blood vessels and not PN axons (see Figure S7). Note that the top and bottom left are at different rostro-caudal positions as indicated in the top left corner of each image. In many cases synaptic terminals can be made out within the individual nuclei (bottom right, corresponds to white box in top image). Dorsolateral Hump of the Interpositus (IntDL), Lateral (Lat), Parvicellular Lateral (LatPC), Superior Vestibular (SuVe), Vestibulocerebellar (VeCb). (B) Confocal micrographs of mossy fiber synaptic terminals labelled with the Vesicular Glutamate Transporter 2 (VGluT2, red) in the MedDL of paired (right) and unpaired (left) mice. (C) The ratio of the number of VGluT2+ puncta in various cerebellar nuclei of paired vs littermate matched unpaired controls. Green bars indicate nuclei in which dye-filled PN axons were detected. Data are represented as mean value ± s.e.m, open circles indicate individual pairs. p values: * < 0.05, ** < 0.01, and ns = no statistical difference.

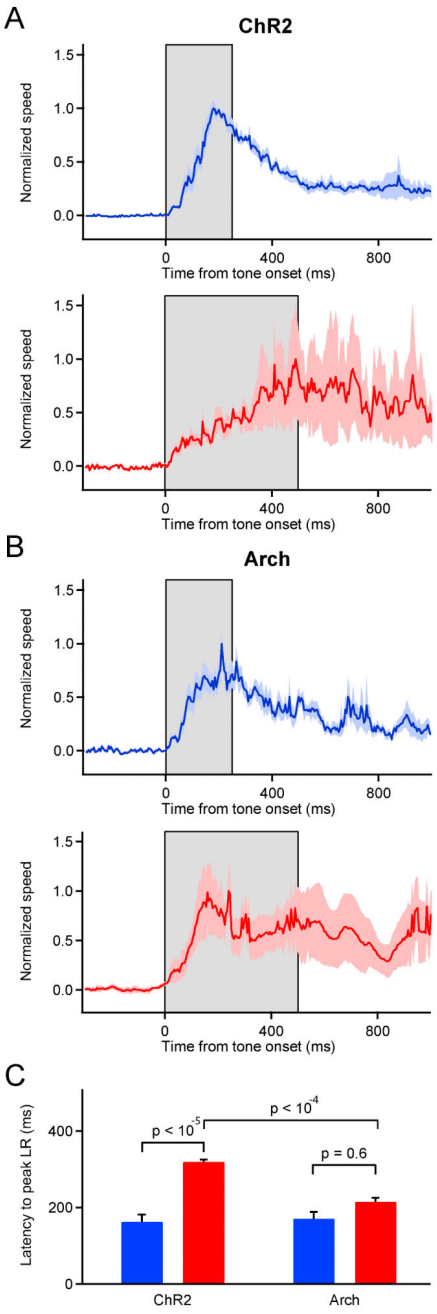

Figure 6. ChR2 training, but not Arch training leads to well-timed, learned movements

(A) Average, normalized movement speed for ChR2 mice in tone-alone LRs occurring between acquisition day 3 and extinction day 1 trained with 250 ms (blue, n = 4 mice) or 500 ms intervals (red, n = 4 mice). Grey boxes indicate intervals between tone and laser pulse onset. Lighter shading represents s.e.m. across mice. (B) Average, normalized movement speed in tone-alone LRs for Arch mice trained with 250 (blue, n = 7 mice) or 500 ms (red, n = 5 mice) intervals. (C) Mean (± s.e.m.) of the delay to the peak LR for all trials included in the averages in A and B. LR timing in ChR2-trained mice is significantly

different between the 250 and 500 ms intervals and between ChR2 and Arch for the 500 ms interval, but not for Arch-trained mice between the 250 and 500 ms intervals. pvalues determined using a two-tailed, Mann-Whitney U test. See also Figure S7 and Table S1.

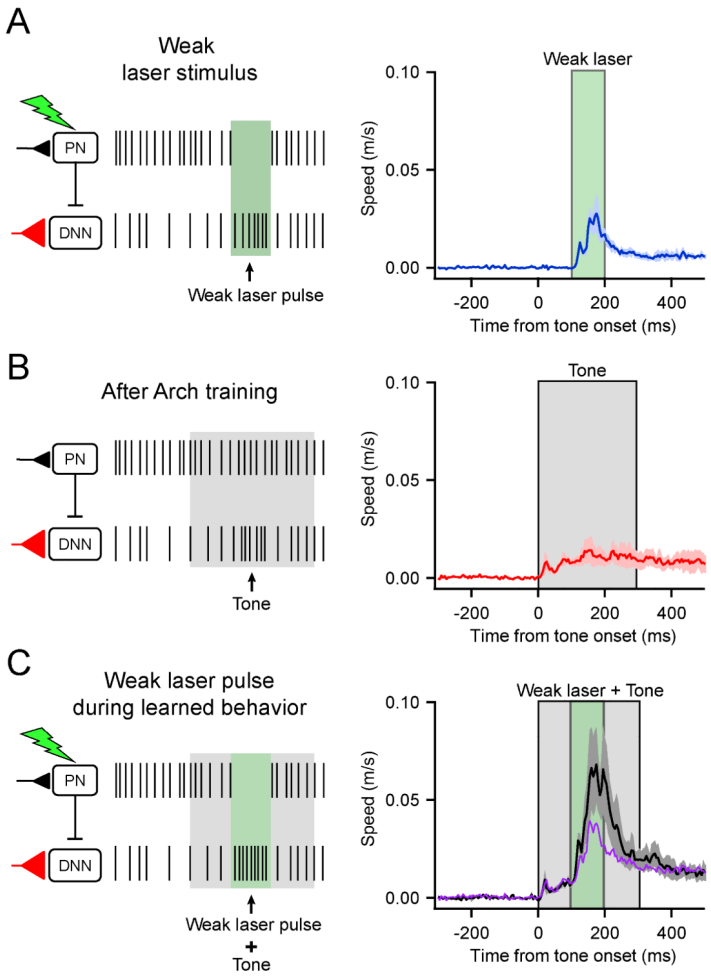

Figure 7. Arch training alters the excitability of CNNs in a tone-dependent manner

Mice were associatively trained by pairing tones and Arch activation as shown in Figure 4. Each panel indicates on the left the hypothesized effects on PN and CNN firing in response to the stimulus and on the right the mean movement speed ± s.e.m. for 3 mice. (A) Mean movements evoked by weak laser pulses. (B) Mean tone-evoked LRs after 4 days of training. (C) Mean movements in response to the tone and weak laser pulse delivered simultaneously. Note that the resulting augmented LRs (black) are larger than the arithmetic sum of the laser-evoked plus the learned movements (purple).

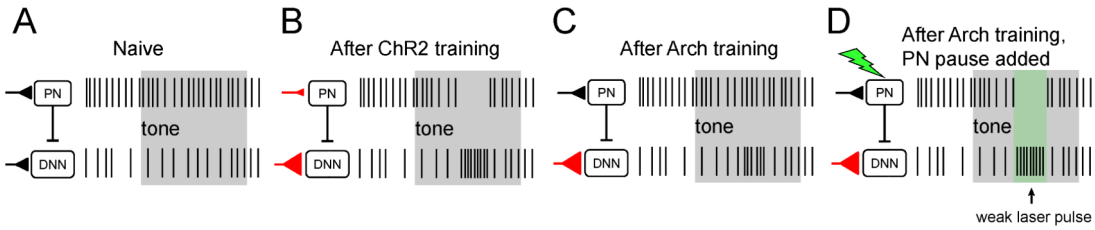

Figure 8. Proposed circuit basis of ChR2- and Arch-driven learning

(A-D) Schematic of proposed model for associative learning in ChR2 and Arch animals. (A) Before learning, the tone (grey box) does not drive activity changes in CNNs. (B) After learning, PNs in ChR2 animals respond with tone-evoked pauses that disinhibit CNNs. Changes in synaptic strength of PN and CNN inputs (red triangles) are hypothesized to underlie learned changes in excitability. (C) After Arch-training, learning results only in increased excitability of CNNs to the learned response. (D) Weak Arch activation (green box), timed to the peak of the forelimb movement mimics disinhibition of CNNs, thereby producing stronger CNN-driven motor output.